THE ASTROPHYSICAL JOURNAL, 489:928–940, 1997 November 10

MAGNETIC FIELD DECAY IN SINGLE RADIO PULSARS: A STATISTICAL STUDY

SOMA MUKHERJEE
Indian Statistical Institute, 203, Barrackpore Trunk Road, Calcutta 700 035, India; soma@isical.ernet.in
AND
AJIT KEMBHAVI
IUCAA, Post Bag 4, Ganeshkhind, Pune 411007, India; akk@iucaa.ernet.in
Received 1996 December 3; accepted 1997 June 24

ABSTRACT

We report on an extensive statistical study of single radio pulsar properties, which we undertook to estimate the decay timescale of pulsar magnetic fields. We synthesized a population of pulsars using assumed theoretical distributions of age, initial magnetic field, period of rotation, position, luminosity, and dispersion measure, taking into account the new distance model for pulsars as well as new velocity estimates. We also took into account the selection effects that characterize pulsar observations. We compared the simulated population with the observed single pulsar population using one- and two-dimensional Kolmogorov-Smirnov tests to obtain a lower bound of ~ 160 Myr on the decay timescale.

Subject headings: pulsars: general — stars: evolution — stars: magnetic fields — stars: rotation

1. INTRODUCTION

Ever since the discovery of pulsars and the development of early theoretical models, there has been much interest and conjecture about the decay of their magnetic fields. Strong magnetic fields are essential in understanding the way pulsars radiate and spin down. Assuming that the observed spin-down is a result of the energy loss due to magnetic dipole radiation, it follows straightforwardly that the surface dipolar fields have a strength of $B_S \sim 10^{12}$ G in young pulsars (Taylor & Stinebring 1986). However, there is no consensus yet on the origin and stability of the magnetic fields. The lack of a fundamental understanding of the pulsar emission mechanism and of the origin of the fields have led to considerable debate regarding the timescale of decay of the magnetic field (Sang & Chanmugam 1990).

In their pioneering statistical study of pulsar properties, Gunn & Ostriker (1970) concluded that pulsar magnetic dipole fields decay on a timescale of $\sim 10^6$ yr. However, this conclusion was based on only about a dozen pulsars on which data were then available. A similar conclusion regarding the temporal behavior of the magnetic fields can be reached by comparing their kinetic age with their spin-down age. The kinetic age is given by $\tau_K \sim z/v_z$, where z is their current distance from the Galactic plane, and v_z is their velocity transverse to it. τ_K corresponds to the time since the formation of the pulsar if it is assumed that pulsars are all formed in the Galactic plane and are ejected with a high velocity relative to it. The other indicator of the age of a pulsar is the spin-down time $P/2\dot{P}$, where P and $\dot{P}$ are the observed period and the period derivative, respectively. This corresponds to the time since formation if it is assumed that the initial spin period $P_i \ll P$ and that the magnetic field is constant. It was noticed that as pulsars aged, the spin-down age lengthened relative to τ_K, which can be interpreted as a decay of the dipole magnetic field (Helfand & Tademaru 1977; Lyne, Anderson, & Salter 1982; Lyne, Manchester, & Taylor 1985). Though a plot, using recent data, of the kinetic age against the spin-down age does show this trend, there is a great deal of scatter, and one can say only that a constant magnetic field definitely seems inconsistent with the distribution of points in the kinetic age/spin-down age plane. Bailes (1989) has subsequently shown that the characteristic age of the low-velocity pulsars is not representative of the time since they acquired the bulk of their velocities, as at that time they possessed spin periods of several hundred milliseconds. Thus the evidence for field decay on the basis of comparison of kinetic and spin-down ages is discredited. Our ignorance about how far from the Galactic plane a pulsar was born, as well as the inability to measure the radial component of the velocity, add to the uncertainty of the results.

On the theoretical side, it has been suggested (Ostriker & Gunn 1969) that the magnetic field should decay from the crust on a timescale of a few million years because of ohmic dissipation of electrical currents in the neutron star. Calculations based on the ohmic decay show that the field cannot decay significantly on the scale of the Hubble time if there is any penetration of the magnetic field lines into the interior of the star (Sang & Chanmugam 1990; Sang & Chanmugam 1987). With realistic thermal evolution and conductivities, isolated neutron stars will maintain large magnetic fields for more than 10^{10} yr (Romani 1990).

Purely observational evidences have also been significant in contributing to the controversy. Discovery of very old neutron stars with substantial field strength in binary pulsars (Bhattacharya et al. 1992, hereafter B92; Bhattacharya & Srinivasan 1991; Bhattacharya & van den Heuvel 1991) and the presence of radio pulsars in globular clusters indicate that the magnetic field of these neutron stars cannot *continue* to decay significantly on the short timescales discussed in the context of young radio pulsars.

Given the uncertain observational and theoretical situation, it is useful to approach the problem of magnetic field decay from a statistical consideration of the large pulsar database that is now available. The idea here is to simulate a population of pulsars from assumed theoretical distributions of various quantities and to subject this set of pulsars to the same observational selection effects as were in operation when real pulsars were discovered in different surveys. This filtered set of pulsars can then be compared with the real population to see whether the simulated and real populations have similar distributions of various parameters such as period, magnetic field, position around the Galaxy, and so on. Parameter values that best reproduce observed

distributions are most likely to be those that occur in the real population. One of the parameters that can be fixed in this manner is the decay timescale for the magnetic field.

A statistical approach of this kind was taken by Narayan & Ostriker (1990), who found that the magnetic field decays on a timescale of ~ 1 Myr. However, in a detailed investigation using the same approach, Bhattacharya et al. (1992) came to the different conclusion that the decay timescale must be at least as long as ~ 100 Myr. Recently Hartman et al. (1997) have obtained a similar result from the simulation of the birth and evolution of radio pulsars throughout the Galaxy. While it has been usual to consider a simple exponential decay model in these calculations, several authors have also performed pulsar statistics with a nonexponential decay model of the magnetic field (Narayan & Ostriker 1990; Wakatsuki et al. 1992). However, such models did not prove to be a marked improvement over the exponential decay model in obtaining a good fit between the observed and simulated data.

In the present paper we closely follow the approach of Bhattacharya et al. (1992) in order to reexamine the issue of the field decay timescale. The new aspects of our study are as follows.

1. We incorporate the most recent catalog of pulsars (Taylor et al. 1995) from the Princeton database, which contains data on 706 pulsars. First, a large database is always helpful in drawing stronger inferences in statistical studies of this nature. More importantly, many of the missing $\dot{P}$ values in the older pulsar catalog (as used in B92) can be obtained in the new catalog.
2. We use a new distance model (Taylor & Cordes 1993) that provides estimates accurate to $\sim 25\%$ or better. The Princeton catalog incorporates the Taylor & Cordes (1993) distance model to calculate the distances of the pulsars.
3. We use the most recent estimate of the mean pulsar birth velocity from direct pulsar proper motion measurements (Lyne & Lorimer 1994).
4. We adopt the Galactic potential discussed in Carlberg & Innanen (1987). This is a three-component axisymmetric model representing the disk/halo, nucleus, and bulge mass distribution in the galaxy (Lorimer 1995).
5. We use two-dimensional Kolmogorov-Smirnov (K-S) tests to compare the distributions of pulsars in the magnetic field–period plane and the period–dispersion measure sin b plane. This has some advantages in sensitivity over the previously used one-dimensional K-S tests, which we also introduce for comparision with previous work.
6. Our simulations span a greater range of values; for example, we vary the decay timescale from 10 Myr to a few hundred million years so that the parameter space is thoroughly tested.
7. We carry out a large number of independent simulations to test the level of statistical noise and the reproducibility of results.

In the following sections we discuss the simulation procedure, the statistical tests involved, and, finally, the results obtained from the analysis.

2. ASSUMPTIONS AND SELECTION CRITERIA USED IN SIMULATIONS

The simulation process for evolving a pulsar from the time of its birth to the present time is based on choosing initial conditions such as the age of the pulsar, the initial surface magnetic field, and the period and the initial position coordinates from appropriate distributions. All other essential properties, such as the magnetic field, luminosity, and flux, can then be calculated from these initial conditions using evolution equations. In the present study, we synthesize a population of single radio pulsars from the assumed theoretical distributions of the properties using Monte Carlo techniques. This is followed by application of selection procedures similar to those that were in effect in the surveys in which pulsars were discovered. The population of these selected pulsars is then compared with the observed population of single radio pulsars.

2.1. *Assumptions*

Age.—The age of a pulsar can be chosen from a uniform distribution between zero and the Hubble time, under the assumption that pulsar birthrate is constant (B92). However, a maximum of 5 times the magnetic field decay constant τ suffices, as any pulsar older than this would evolve beyond the death line. Thus,

$$t \sim U(0, 5\tau) , \tag{1}$$

i.e., the age is chosen from a uniform distribution between 0 and 5τ. However, the assumption that the pulsar birthrate is constant is not a foolproof one. This will be discussed in § 6.

Magnetic field.—The initial magnetic field strength B_i is chosen from a normal distribution in $\log B_i$, i.e.,

$$p(\log B_i)d(\log B_i) = \frac{1}{\sqrt{2\pi}\sigma_{\log B_0}} \times \exp\left[\frac{-(\log B_i - \log B_0)^2}{2\sigma^2_{\log B_0}}\right] d(\log B_i) . \tag{2}$$

The mean value and the dispersion that define the distribution are to be determined from the comparision of the simulated and observed populations as described below. Following general practice, we assume that the magnetic field has an exponential time dependence:

$$B(t) = B_i \exp\left(-\frac{t}{\tau}\right) . \tag{3}$$

Period.—The period of rotation is calculated from its relation to the magnetic field using the standard dipole rotator model (Gunn & Ostriker 1970):

$$P\dot{P} = \frac{8\pi^2 R^6}{3Ic^3} B^2 , \tag{4}$$

where $R = 10^6$ cm is the radius and $I = 10^{45}$ g cm^2 is the moment of inertia of the neutron star. The initial period is taken to be fixed at a value $P_i = 0.1$ s because, as explained in Bhattacharya et al. (1992), pulsars with an initial period less than this value evolve to it on a timescale negligible compared to the age of the pulsars as considered in this simulation.

Beaming fraction.— For a pulsar to be observable, the pulsar beam should intersect the line of sight to an observer on Earth. The fraction of the sky covered by a pulsar beam depends on its period of rotation. We have used the beaming function f_b as modeled by Narayan & Vivekanand (1983) and Rankin (1990). It is given by

$$f_b \sim P^{-1/2} \tag{5}$$

for $P \geq 0.1$ s. We have independently done the calculation relating f_b and P using nonlinear regression methods to

re-establish the $P^{-1/2}$ dependence and determine the constant of proportionality in the process. The expression obtained by us is given by

$$f_b = 0.36075 \times P^{-0.45928} \quad (6)$$

for $P \geq 0.1$ s. For pulsar periods that led to $f_b < 0.2$, we set $f_b = 0.2$. Using other laws (Lyne & Manchester 1988) to relate f_b and P does not significantly affect our results.

Position.—The radial position R_i of a pulsar in the Galactic plane, in Galactocentric coordinates, is chosen from a normal distribution (Narayan 1987) given by

$$p(R_i)dR_i = \frac{1}{\sqrt{2\pi R_0^2}} \exp\left(\frac{-R_i^2}{2R_0^2}\right) dR_i \, . \quad (7)$$

The Galactocentric radius of the Sun is assumed to be 8.5 kpc, and the disk scale length R_0 is 4.8 kpc. Only those pulsars were retained in our simulation for which the heliocentric distance was found to be less than 3 kpc. This is done in order to keep the selection effects in our simulation similar to those of B92 for comparison of results. Increasing this distance adds just a few observed pulsars to the sample, when all other selection criteria are applied (see below), while considerably increasing the required computing time.

The initial height of the pulsar above (or below) the Galactic plane is chosen from an exponential distribution with scale height h of the pulsar progenitors (Mihalas & Binney 1981):

$$p(z_i)dz_i = \frac{1}{2h} \exp\left[-\frac{|z|}{h}\right] dz_i \, . \quad (8)$$

Following B92, we have chosen $h = 0.06$ kpc.

The initial velocity, v_{z_i}, of the pulsars in the vertical direction was chosen from a Gaussian distribution with mean $\langle v_{z_i} = 0 \rangle$ and dispersion $\sigma_v = 200$ km s^{-1} (Lyne & Lorimer 1994, 1995):

$$p(v_{z_i})dv_{z_i} = \frac{1}{\sqrt{2\pi}\sigma_v} \exp\left[-\frac{1}{2}\frac{v_{z_i}^2}{\sigma_v^2}\right] dv_{z_i} \, . \quad (9)$$

New determinations of proper motion (Harrison, Lyne, & Anderson 1993) and the new electron density model of Taylor & Cordes (1993) have led to a re-estimation of the velocities of pulsars. The present estimate of $\sigma_v = 200$ km s^{-1} exceeds the value of 110 km s^{-1} used by B92 because the old distance model (Lyne et al. 1985) used in their paper underestimated the distance to nearby pulsars and also because of the discovery of a number of young and higher velocity pulsars in recent astrometric surveys (Harrison et al. 1993; Fomalont et al. 1992).

The simulated pulsars were allowed to move under the Galactic potential given by Carlberg & Innanen (1987) (see Lorimer 1995). This is a three-component, axisymmetric model representing the disk/halo ($\Phi_{\rm DH}$), nucleus ($\Phi_{\rm nuc}$), and bulge mass ($\Phi_{\rm bul}$) distribution in the Galaxy. The total Galactic potential is the sum of these three contributions:

$$\Phi_{\rm gal} = \Phi_{\rm DH} + \Phi_{\rm nuc} + \Phi_{\rm bul} \, . \quad (10)$$

The disk/halo potential is given by

$$\Phi_{\rm DH}(R, z) = -\frac{GM}{\sqrt{[a + \sum_{i=1}^{3} \beta_i (z^2 + h_i^2)^{1/2}]^2 + b^2 + R^2}} \, , \quad (11)$$

where M is the disk/halo mass, a and h are the scale length and scale height of the disk, respectively, and b is the core radius of the halo. The summation refers to old disk, dark matter, and young disk contributions. The β_i are proportionality factors. For the nucleus and the bulge contributions, the scale height terms are set equal to zero so that the form of the potential for these contributions becomes

$$\Phi_{\rm nuc} = \Phi_{\rm bulge} = -\frac{GM}{\sqrt{b^2 + R^2}} \, . \quad (12)$$

The values of a, b, h, and the β_i are obtained from Table A.1 in Lorimer (1995). The Galactocentric radius, R, is taken to be equal to $(x^2 + y^2)^{1/2}$ and is generated from a normal distribution as described above. The circular rotation speed on the Galactic plane, $v_{\rm rot}$, is obtained from the centrifugal force per unit mass and the gravitational force per unit mass experienced by a test particle in a gravitational field. It is given by

$$v_{\rm rot}(R) = \left[R \frac{\partial}{\partial R} \Phi_{\rm gal}(R, 0)\right]^{1/2} \, . \quad (13)$$

The circular rotation speed, $v_{\rm rot}$, is vectorially added to the components of velocity generated from the normal probability distribution described above. For the present study, only the vertical motion of the pulsar is followed keeping x and y constant, as will be explained in more detail in § 5.

Luminosity at 400 MHz.—It is possible to determine the luminosity of a pulsar from its period and period derivative. A model to determine the 400 MHz luminosity has been provided by Proszynski & Przybycien (1984) and Narayan (1987) and is given by

$$\log \langle L_{400} \rangle_0 = 6.64 + \frac{1}{3} \log \frac{\dot{P}}{P^3} \, , \quad (14)$$

where the units of luminosity are mJy kpc^2. In an alternative model by Stollman (1986), the expression relating the variables is

$$\log \langle L_{400} \rangle_0 = (-10.05 \pm 0.84) + (0.98 \pm 0.03) \log \frac{B}{P^2} \, ,$$

$$\log \frac{B}{P^2} \leq 13 \quad (15)$$

and

$$\log \langle L_{400} \rangle_0 = 2.71 \pm 0.60 \, , \quad \log \frac{B}{P^2} > 13 \, . \quad (16)$$

These relations are based on the distribution of observed luminosity and provide the mean luminosity of a population. The observations, and therefore the mean, are, however, biased toward the higher luminosities. The distribution of the *intrinsic* luminosity around the mean has been modeled by Narayan & Ostriker (1990) and is given by

$$\rho(\lambda) = 0.5\lambda^2 e^{-\lambda} \, , \quad (17)$$

where

$$\lambda = a\left(\log \frac{L_{400}}{\langle L_{400} \rangle_0} + b\right) , \quad (18)$$

with $a = 3.6$ and $b = 1.8$ for Proszynski & Przybycien's law and $a = 3.0$ and $b = 2.0$ for the Stollman luminosity law.

The procedure adopted in the simulations is to determine the mean luminosity given P and $\dot{P}$ and then to pick at random a luminosity from the distribution around this mean. Both of the luminosity laws were used for the goodness-of-fit tests that followed the simulations.

Determination of flux.—The flux in mJy received from a pulsar at 400 MHz is given by

$$S_{400} = \frac{L_{400}}{x^2 + y^2 + z^2} . \tag{19}$$

Calculation of the limiting flux.—Corresponding to the observation in a given direction in a given survey, there is a limiting flux $S_{\min}$ below which the detection of the pulsar is not guaranteed. In order to ensure completeness of the survey, it is necessary to retain only those pulsars that have flux greater than $S_{\min}$. This limiting flux, $S_{\min}$, is a function of period, dispersion measure, and instrument-specific parameters. We have used the detection criteria of one of the four major pulsar surveys conducted at 400 MHz: the Jodrell Bank survey (Davies, Lyne, & Seiradakis 1972), the University of Massachusetts–NRAO survey (Damashek, Taylor, & Hulse 1978), the University of Massachusetts–Arecibo survey (Hulse & Taylor 1974), and Second Molonglo survey (Manchester et al. 1978).

The dispersion measure can be calculated from the distance of the pulsar and the electron density at that specified location. We have adopted the new distance model (Taylor & Cordes 1993) that incorporates the effects of Galactic spiral arms, the shapes and locations of which are derived from the radio and optical observations of H II regions. The model also includes the electron densities of the outer and inner axisymmetric components and of spiral arms, with appropriate scale lengths and fluctuation parameters used to relate the dispersion and scattering contributions of the features. Owing to its large angular size and proximity, the Gum Nebula is also a significant contributing factor to the dispersion measure.

The electron density of a specified Galactic location is defined as the sum of contributions from each of the four components:

$$n_e(x, y, z) = \sum_{i=1}^{2} n_i g_i(r) \operatorname{sech}^2\left(\frac{z}{h_i}\right) + n_a \operatorname{sech}^2\left(\frac{z}{h_a}\right) \times \sum_{j=1}^{4} f_j g_a(r, s_j) + n_{\mathrm{Gum}} g_{\mathrm{Gum}}(u) , \tag{20}$$

where $r = (x^2 + y^2)^{1/2}$. The summation is taken over the four spiral arms. The f_j are scale factors connected to the spiral arms. The functions g_1, g_2, g_a, and g_{Gum} signify position dependences of the model. The values of the parameters of the model can be found in Taylor & Cordes (1993).

The dispersion is obtained from the relation

$$\mathrm{DM} = \int_0^d n_e \, ds . \tag{21}$$

We have used the Fortran subroutine provided by Taylor & Cordes (1993) to calculate the dispersion measure.

The contribution of scatter broadening to the pulse width is given by

$$\tau_{\mathrm{scatt}} = 10^{-4.62 \pm 0.52 + (1.14 \pm 0.53) \log \mathrm{DM}} + 10^{-9.22 \pm 0.62 + (4.46 \pm 0.33) \log \mathrm{DM}} . \tag{22}$$

The cumulative distribution of $\Delta \log \tau$ is represented very well by the function $\{1 + \exp [(x_0 - \Delta \log \tau)/a_0]\}^{-1}$, with $x_0 = 0.04$ and $a_0 = 0.342$ (B92).

The final width of the broadened pulse is given by (Narayan 1987)

$$W^2 = W_e^2 + \tau_{\mathrm{samp}}^2 + \tau_{\mathrm{DM}}^2 + \tau_{\mathrm{scatt}}^2 , \tag{23}$$

where τ_{samp} is the broadening caused by the finite sampling time of the data, τ_{DM} is due to dispersion smearing, and W_e is the width of unbroadened pulse. The variable $\tau_{\mathrm{DM}} = C_{\mathrm{DM}} \mathrm{DM}$, where C_{DM} is a constant. The values of C_{DM} and τ_{samp} for the pulsar surveys used in the present study are given in Narayan (1987). The minimum flux is then obtained from

$$S_{\min} = S_0 \left(\frac{T_r + T_{\mathrm{sky}}}{T_0}\right) \left[\frac{PW}{W_e(P - W)}\right]^{1/2} , \tag{24}$$

where S_0 is the survey flux limit, T_r is the receiver excess noise temperature, T_{sky} is the sky background temperature, and T_0 is a normalization constant. All the parameter values can be obtained from Haslam et al. (1982), Dewey et al. (1984), and Narayan (1987).

2.2. *Selection Criteria*

After a pulsar is generated with parameters chosen at random from their known distributions, one has to make sure that the pulsar would actually be observed in at least one of the surveys used in forming the observed ensemble of pulsars that is used in the comparision. For it to be detected, a pulsar must have the right combination of period and field strength so as to lie above the death line and should be beamed toward the Earth. Also, the flux measured should lie above a limiting flux as described above. Our simulated pulsars were subjected to the selection criteria described below, so that the accepted set resembles the set of observed pulsars as closely as possible. A comparision between simulated and observed populations then becomes meaningful, since both the populations suffer from the same selection effects.

First selection criterion.—A pulsar is retained in the simulation only if it lies above the death line (Ruderman & Sutherland 1975; Rawley, Taylor, & Davis 1986), i.e., it satisfies the condition

$$\frac{B}{P^2} > 0.17 \times 10^{12} \ \mathrm{G \ s^{-2}} . \tag{25}$$

Second selection criterion.—We have seen in equation (6) how the fraction of the sky covered by a pulsar beam is related to its spin period. We have to make sure that for a pulsar to be a part of the observed sample, the beam intersects the line of sight. For a randomly oriented pulsar, the probability that this happens is proportional to the beamwidth. Having obtained f_b from P, we selected a random number u (say), and if the condition $u \leq f_b$ was satisfied, we retained the pulsar in the simulation; otherwise, we rejected it. This ensures that, of the pulsars that we begin with, we retain only the fraction warranted by the beamwidth.

Third selection criterion.—We have used observed pulsars that have been found in at least one of the four major surveys conducted at 400 MHz, viz. the Jodrell-Bank survey, the University of Massachusetts–Arecibo survey, the Second Molonglo survey, and the University of

Massachusetts–NRAO survey. Every simulated pulsar that is included in the sample should therefore be detectable in at least one of these surveys and meet the selection criterion for completeness, i.e.,

$$S_{400} \geq S_{\min} . \quad (26)$$

3. SAMPLE SELECTION FROM REAL PULSARS

The data for real pulsars were obtained from the catalog of 706 pulsars from the Princeton database (Taylor et al. 1995). We dropped binaries, supernova remnants, and X-ray and γ-ray pulsars and isolated a subset of 511 single radio pulsars. An additional 43 pulsars had to be dropped from the population because of missing $\dot{P}$ values. The remaining population of pulsars was then passed through the same selection effects as those used for the simulated population, since the models and survey parameters used for the calculation of $S_{\min}$ in § 2 give only an approximate minimum flux for which the surveys were reasonably complete, rather than an absolute minimum flux (B92). This led to the retention of only 97 pulsars from the observed sample.

Figure 1 shows the distribution of the age, vertical component of dispersion measure, flux, magnetic field, period, and period derivative of the observed set of 478 pulsars (*dotted lines*) and of the selected pulsars (*solid lines*).

4. STATISTICAL TESTS

The simulated population depends on a number of assumptions and values for parameters. However, the most important parameters in our simulation are just three: the decay timescale τ, $\log B_0$, and the variance $\sigma^2_{\log B_0}$. For a given simulation, we assume a luminosity law and generate a sequence of populations by allowing $\log B_0$, $\sigma^2_{\log B_0}$, and τ to vary in suitable steps.

For each choice of parameters, we have used the Kolmogorov-Smirnov test in its standard one-dimensional form and a generalization to two dimensions to compare the simulated and observed populations. We run through the range of parameters, generate a simulated and selected sample for each set of parameter values, and make the comparision. The aim of this procedure is to determine the

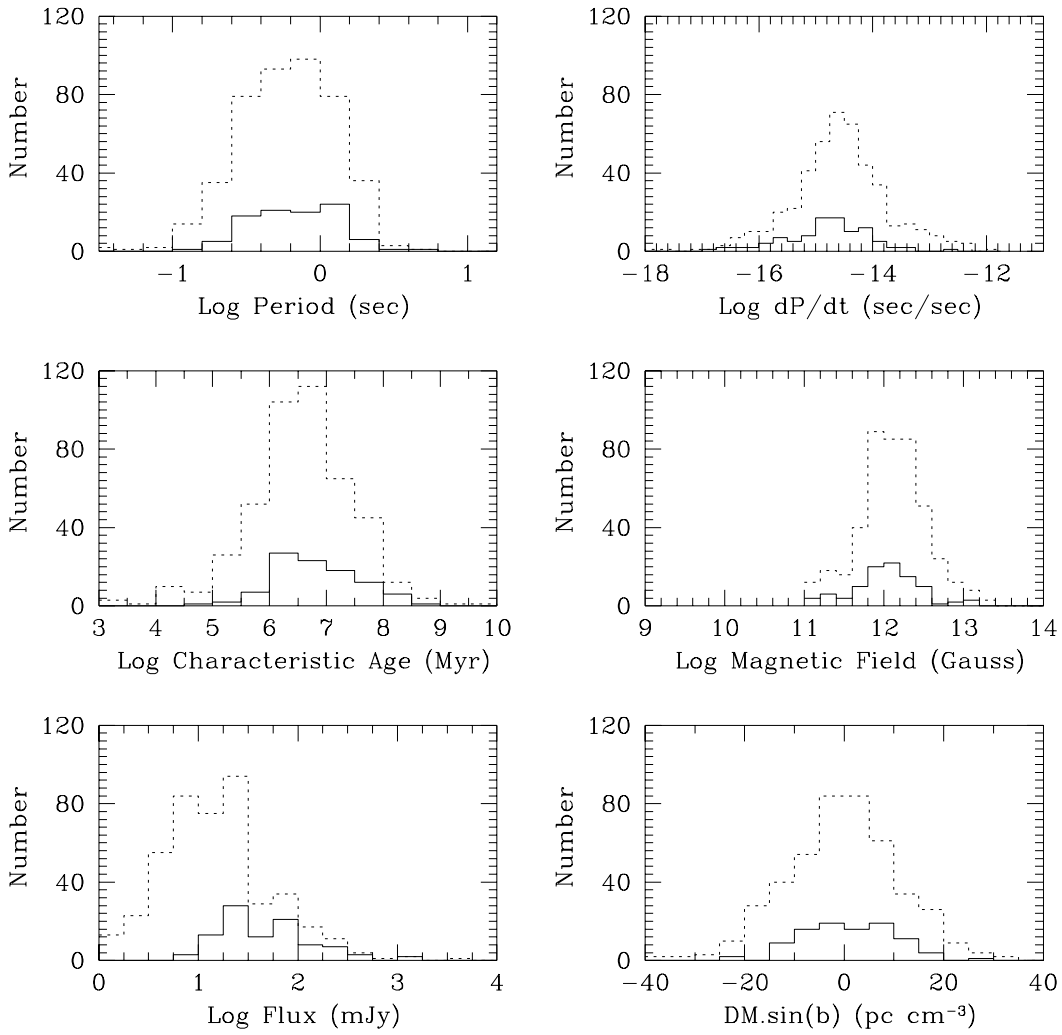

FIG. 1.—Distribution of various pulsar properties before and after selection. The dotted lines show the distribution for all observed single radio pulsars for which we have all the required data, and the solid lines show the distribution after selection criteria are applied to the observed population, as explained in the text.

parameter values for which we get the best match between the simulated and the real populations. The value of τ for which we get this match gives an estimate of the magnetic field decay timescale for the population of single radio pulsars.

4.1. *The One-dimensional Kolmogorov-Smirnov Statistic*

The degree of similarity between the simulated and observed populations can be ascertained by comparing the distribution of various attributes of individual pulsars, such as the period and magnetic field for the two populations. The one-dimensional K-S test provides a simple measure of the overall difference between two distributions. The K-S statistic is defined as (see Press et al. 1992 for a brief discussion)

$$D = \max | S_{N_1}(x) - S_{N_2}(x) | , \tag{27}$$

where $S_{N_1}(x)$ and $S_{N_2}(x)$ are two cumulative probability distribution functions of the parameter x. N_1 and N_2 are the number of objects in the two samples, respectively. The one-dimensional test does not depend in any way on the shape of the parent distribution and does not require any binning of the data.

The K-S probability can be obtained for each of the independent attributes that define the population. The three parameters we use are the period, P, the magnetic field, B, and the vertical component of the dispersion measure, DM $\sin | b |$, as these can be independently specified for each pulsar. Battacharya et al. (1992) also use luminosity as an independent attribute, but we find that it is not necessary to include it in the tests. The luminosity of each pulsar can be obtained as described above, given a law that determines mean luminosity, as in equation (15), for instance, and the distribution of individual luminosity about the mean, which has the fixed form given in equations (17) and (18). It is therefore not an independent parameter. We have verified that the conclusions we reach about the population are independent of whether or not the luminosity is used as an extra attribute in the comparision, and we do not consider it any further.

From the individual probabilities for the three attributes P, $\dot{P}$, and DM $\sin | b |$, we obtain an overall probability, which is the product of the three probabilities, and use it as the indicator of the degree of similarity in the distributions. We vary the three parameters $\log B_0$, $\sigma_{\log B_0}$, and τ in the manner described above and find the combination for which the maximum product probability is obtained.

4.2. *The Two-dimensional Kolmogorov-Smirnov Statistic*

In the one-dimensional K-S test, the distribution of each attribute in the simulated and real populations is compared independently from the distributions of the other attributes. However, it would be most natural to consider the joint distribution of the triplet (P, $\dot{P}$, DM $\sin | b |$) for the two populations. While this would be difficult to do computationally, schemes have been developed for comparing two-dimensional distributions (Peacock 1983; Fasano & Franceschini 1987; see Press et al. 1992 for a brief description and numerical algorithms of the Fasano & Franceschini version), which are analogous to the Kolmogorov-Smirnov test applicable in one dimension and are loosely termed as two-dimensional K-S tests. In our case, the three attributes can be divided into the two planes (P, $\dot{P}$) and (P, DM $\sin | b |$), and the distributions in these planes of the simulated and real pulsars can be considered.

We adopt Fasano & Franceschini's (1987) version of the two-dimensional K-S test. In this test, the absolute difference between the observed and the predicted (normalized) two-dimensional cumulative distributions is computed separately in the four quadrants of the plane defined by the variables of interest. Thus, for any data point with coordinates (X_i, Y_i), the observed data and predictions are summed up in the four quadrants of the plane defined by

$$(x < X_i, y < Y_i) , \quad (x < X_i, y > Y_i) , \quad (x > X_i, y < Y_i) ,$$
$$(x > X_i, y > Y_i) , \quad i = 1, \ldots, n . \tag{28}$$

The statistic $D_{\text{K-S2}}$ is taken to be the *largest* of the differences of the integrated probabilities when all data points are considered. The probability that a difference exceeding $D_{\text{K-S2}}$ is obtained under the null hypothesis is approximately given by Press et al. (1992).

We evaluate the two-dimensional K-S probability for distributions in the (P, B) and (P, DM $\sin | b |$) planes and, as in the one-dimensional case, obtain the product probability. We will see that this appears to provide a better discriminant than the one-dimensional product probability. We shall compare the relative merits of the one-dimensional and two-dimensional tests in detail in a future publication.

4.3. *Parameter Ranges*

As explained at the beginning of this section, the variable parameters in our simulations are (1) the magnetic field decay constant, τ; (2) the mean of the logarithm of the initial magnetic field, $\log B_0$; and (3) its variance, $\sigma_{\log B_0}$. In order to determine the optimum step size of these parameters and the number of objects to be used in the simulation, we first generated a "real population" using some set of input parameters and tried to recover these through the process of simulation and comparision using the K-S test.

We began by varying τ from 10 to 370 Myr in steps of 10 Myr, $\log B_0$ from 12.0 to 13.0, and $\sigma_{\log B_0}$ from 0.2 to 0.4, both in steps of 0.01. We found that the K-S probability values were insensitive to such small step variations of $\log B_0$ and $\sigma_{\log B_0}$ and showed fluctuations. By increasing the step size and repeating the simulations several times, we found that step sizes of 0.1 for $\log B_0$ and $\sigma_{\log B_0}$ and 30 Myr for τ led to stable probabilities, and peak probabilities were always obtained for the values of parameters that were equal to the input values.

If too few simulated pulsars are used in the comparision with the observed population, the results obtained will change owing to "noise" from one set of simulated pulsars to another. On the other hand, if the simulated set is very large, the requirement on computer time will be prohibitive. In order to decide on the size of the simulated sample, we again had trial runs with samples of 200 and 2000 objects each and tried to recover known input values that went into defining a "real population." We found that with 2000 simulated pulsars, the input parameter values could always be recovered, independent of the seed value used in random number generation for simulating a population. However, when the same tests were carried out with 200 simulated pulsars, we observed unacceptable fluctuations in the probability values for test runs with different seeds. Therefore, in all the simulations that followed, we kept the sample size of the simulated pulsars at 2000. Nevertheless, test runs with

the smaller number provided valuable insights during the early stages of the project.

As explained above, the simulation procedure involves choosing pulsars with parameters that are picked at random from certain distributions and then passing them through selection filters to ensure that the simulated objects could actually be observed on Earth under the conditions of the discovery surveys. When survey conditions were not met, the pulsar had to be dropped from consideration. The rejection level of simulated pulsars because of the imposition of selection effects was quite high: in order to obtain 2000 simulated pulsars that satisfied the selection effects, we found it was necessary to make $\sim 10^6$ trials, i.e., only one of every ~ 500 simulated pulsars could meet the selection criteria of at least one of the four surveys from which our observed sample was derived. The requirement that the calculated flux should be above a minimum limiting flux led to maximum rejection.

We found that in all trial cases of comparision between simulated and observed pulsars, maximum probability values were obtained for $\log B_0$ in the range 12.3–12.5 and $\sigma_{\log B_0}$ in the range 0.3–0.5. In order to reduce the computer time needed, we restricted the variation in these parameters to these short ranges. We ensured from time to time that probability maxima were not situated outside these ranges by having runs over wider ranges.

5. RESULTS OF SIMULATIONS

In the simulations reported here we have considered pulsar motion only in the direction normal to the Galactic plane, after obtaining their initial positions in the plane using the appropriate probability distribution. We assume that the velocity dispersion for the pulsars is 200 km s^{-1}. Evolution of pulsar positions by considering their motion in three dimensions slows down the simulation process considerably. We have made some preliminary simulation studies with three-dimensional motion taken into account, and the results support the conclusions reported in this paper. We shall present details of these simulations in a later work.

We have performed the one- and two-dimensional K-S tests between the simulated and observed samples by varying $\langle \log B_0 \rangle$ from 12.0 to 12.3 in steps of 0.1, $\sigma_{\log B_0}$ from 0.3 to 0.5 in steps of 0.1, and τ from 10 to 370 Myr in steps of 30 Myr. We have used the luminosity laws of Stollman (1986) as well as Proszynski & Przybycien (1984) in order to arrive at the best-fit model. Our samples of simulated and selected pulsars always have 2000 objects.

When the mean and dispersion in the initial magnetic field are varied over their range, we find that the best fit, i.e., the maximum product probability, is always obtained for $\log B_0 = 12.4$ and $\sigma_{\log B_0} = 0.4$. We have presented in Table 1 the results of one- and two-dimensional K-S tests when the decay constant was varied over its range, with $\log B_0$ and $\sigma_{\log B_0}$ held fixed at 12.4 and 0.4, respectively. Three sets of values of the one- and two-dimensional K-S probabilities corresponding to three sets of simulations with different seed values are listed. The table shows results for the luminosity laws of Stollman (1986) as well as those of Proszynski & Przybycien (1984).

It is seen from Table 1 that for low values of τ, the simulations poorly reproduce the observed distributions. Probabilities are very low for values of τ up to 100 Myr. However, beyond $\tau = 160$ Myr, there is a distinct rise in the probability values (by a factor of $\sim$2–4), which tend to reach saturation for $\tau > 220$ Myr. It is important to note that in the case of the one-dimensional K-S test, probability values for $\tau > 160$ Myr can occasionally drop to values comparable to those corresponding to ≤ 100 Myr. However this is *never* so with the two-dimensional K-S probability. Even though there is statistical fluctuation in the probability values for $\tau \geq 220$ Myr, the values at any stage beyond $\tau \geq 220$ Myr never approach values corresponding to $\tau \leq 100$ Myr.

We have shown in Table 2 the peak K-S probabilities and the corresponding τ values obtained for many runs, each

TABLE 1

ONE- AND TWO-DIMENSIONAL K-S PRODUCT PROBABILITIES

		SIMULATION 1		SIMULATION 2		SIMULATION 3	
LUMINOSITY LAW	τ (Myr)	$P^{1D}_{\rm product}$	$P^{2D}_{\rm product}$	$P^{1D}_{\rm product}$	$P^{2D}_{\rm product}$	$P^{1D}_{\rm product}$	$P^{2D}_{\rm product}$
Stollman.....	10	8.3E−8	1.5E−9	3.2E−8	1.18E−10	8.5E−9	8.6E−11
	40	4.9E−4	5.2E−5	6.8E−3	1.4E−4	4.0E−4	4.9E−5
	70	0.001	0.001	9.5E−4	1.8E−4	0.002	8.0E−4
	100	0.008	0.005	0.013	0.010	0.007	0.009
	160	0.015	0.022	0.007	0.020	0.021	0.032
	220	0.019	0.024	0.014	0.013	0.006	0.017
	250	0.019	0.025	0.020	0.020	0.011	0.026
	280	0.017	0.034	0.013	0.022	0.009	0.014
	310	0.030	0.035	0.022	0.015	0.018	0.032
	370	0.023	0.035	0.069	0.050	0.041	0.072
Proszynski & Przybycien.....	10	4.7E−7	9.9E−9	1.1E−7	9.8E−10	4.7E−7	9.9E−9
	40	6.4E−4	2.6E−4	1.3E−4	1.3E−4	6.4E−4	2.6E−4
	70	6.0E−4	2.6E−4	6.2E−4	0.001	5.8E−4	2.0E−4
	190	0.002	1.4E−4	7.3E−4	6.9E−5	0.002	1.4E−4
	310	0.006	7.7E−4	0.005	2.2E−4	0.006	7.7E−4
	340	0.007	2.9E−4	0.004	3.3E−4	0.007	2.9E−4
	370	0.019	0.002	0.014	0.001	0.019	0.002

NOTE.—For different values of decay timescales for $\log B_0 = 12.4$ and $\sigma_{\log B_0} = 0.4$. The pulsar motion is assumed to be normal to the Galactic plane, with a velocity dispersion of 200 km s^{-1}. The K-S probabilities for three sets of simulations corresponding to different seed values are shown. The number of selected pulsars in each run is 2000.

TABLE 2

ONE- AND TWO-DIMENSIONAL K-S BEST-FIT VALUES CORRESPONDING TO PEAK PRODUCT PROBABILITIES

	ONE DIMENSION		TWO DIMENSIONS	
LUMINOSITY LAW	τ	$P^{1D}_{\rm product}$	τ	$P^{2D}_{\rm product}$
Stollman	340	0.029	250	0.044
	280	0.033	190	0.040
	220	0.045	220	0.060
	310	0.035	310	0.056
	370	0.049	370	0.057
	310	0.052	310	0.090
	250	0.043	160	0.066
	220	0.034	310	0.054
	250	0.026	310	0.060
	370	0.041	370	0.072
	310	0.029	370	0.036
	250	0.048	340	0.066
Proszynski & Przybycien	160	0.013	160	0.010
	310	0.011	100	0.010
	340	0.009	220	0.010
	370	0.017	130	0.019
	280	0.018	100	0.018
	250	0.016	340	0.011

NOTE.— Each entry for τ is the decay timescale for which the maximum product probability is obtained, in a run with τ varying over the range 10–370 Myr, log B_0 varying between 12.3 and 12.5, and $\sigma_{\log B_0}$ varying between 0.3 and 0.5. In every run the maximum was obtained for log $B_0 = 12.4$ and $\sigma_{\log B_0} = 0.4$, so all entries shown are for these values. Other assumptions are as in Table 1.

initiated with a different seed value. For each seed value, the parameters log B_0, $\sigma_{\log B_0}$, and τ were varied over their respective ranges, which were mentioned above. Since in every run the maximum probability was obtained for log $B_0 = 12.4$ and $\sigma_{\log B_0} = 0.4$, these values are not separately indicated in the table. It is seen from the table that in every run the best fit was obtained for $\tau \geq 160$ Myr, even though τ was varied over a wide range.

It is seen from both Tables 1 and 2 that the probabilities obtained in the simulations carried out with Stollman's luminosity law are always greater than those corresponding to Proszynski & Przybycien's luminosity law. Stollman's luminosity law therefore provides a better overall fit between simulated and observed pulsars. This is true for both one- and two-dimensional K-S tests.

The values of τ corresponding to the best fit varied from 160 to 370 Myr in the different sets of simulations using different initial seed values. It is important to note that even though we have repeated the entire procedure several times using different seed values, *in none of the cases* do we obtain the best-fit model for values of $\tau < 160$ Myr, though the starting value in our simulation loop for τ is 10 Myr. This consistently sets a *lower bound* to the value of τ, which shows that the existing model favors a longer value of the magnetic field decay constant. This is equally true for one-dimensional as well as two-dimensional tests.

Figure 2 illustrates the above results explicitly through equal probability contours. The contours in each panel show the locus of equal probability points as log B_0 and the magnetic field decay timescale, τ, are varied. In each panel contours for $\sigma_{\log B_0} = 0.3$ and 0.4 are shown. The four panels correspond to two different seed values for the random number generators used in the simulations and one- and two-dimensional K-S tests. Results shown are for Stollman's luminosity law and a velocity dispersion $\sigma_v = 200$ km s^{-1}. The figure shows the sensitivity of the probability to variations of different parameters. The vertically elongated nature of the contours indicates that the probabilities are more sensitively dependent on the initial magnetic field value than the decay timescale. The dots in each panel show the maximum probability, and it is clear that the maximum in every case occurs at log $B_0 = 12.4$ and $\sigma_{\log B_0} = 0.4$. While the position of highest probability on the τ-axis depends on the other parameters, it is always high, which indicates that there is almost no field decay during the lifetime of the pulsar.

Another point of interest in Table 2 is that the maximum two-dimensional product probabilities are *always* greater than the corresponding one-dimensional product probabilities, which indicates that the two-dimensional test provides a better way to discriminate between the different sets of input parameter values so as to obtain the best-fit model. This also shows that a *multiparameter* comparison of the simulated and observed pulsars is better brought out by testing the distributions in the parameter space by using a higher dimensional K-S test than by using the one-dimensional K-S test to compare the properties individually.

Figure 3 shows the distributions of the observed pulsars against the simulated pulsars corresponding to log $B_0 = 12.4$, $\sigma_{\log B_0} = 0.4$, and $\tau = 280$ Myr. The distributions shown are for period, period derivative, the magnetic field, DM sin b, and the luminosity at 400 MHz. The close coincidence of the distributions of the simulated and the observed pulsars show that our simulations can reproduce the actual observed distribution of the respective properties of the pulsars well. Figures 4 and 5 show the cumulative distribution of the pulsars for the period, the period derivative, the magnetic field, and the luminosity for two values of τ, viz. 280 and 10 Myr. It is quite clear from the figures that the simulated pulsars follow the observed pulsar distribution closely for $\tau = 280$ Myr, but show a rather poor fit for $\tau = 10$ Myr. Figure 6 shows the distribution of the pulsars in the B-P plane.

6. DISCUSSION

Though we began with an observed sample of 467 pulsars, for each of which we had all the information necessary to do our tests, the selection effects lead to the retention of only 97 pulsars in our sample. We have found that most of the rejection occurs because the observed flux falls below the minimum flux calculated on the basis of the model based on survey parameters. However, rejection of so many *observed* pulsars for this reason implies that all assumptions in the model for the calculation of $S_{\rm min}$ should be thoroughly checked, and a better model, which can give a more realistic minimum flux estimate, should be developed such that fewer observed pulsars are deleted from the sample.

The selected pulsars tend to have their luminosity toward the higher values of the luminosity distribution of the full sample. This happens because of the minimum flux selection criterion. However, the distributions of all other parameters are similar for the selected subsample and the full observed sample.

The main goal that we have addressed in this paper is to find a good estimate of the magnetic field decay timescale. Our simulations have consistently shown that the best-fit models correspond to $\tau \geq 160$ Myr. In fact it can be seen

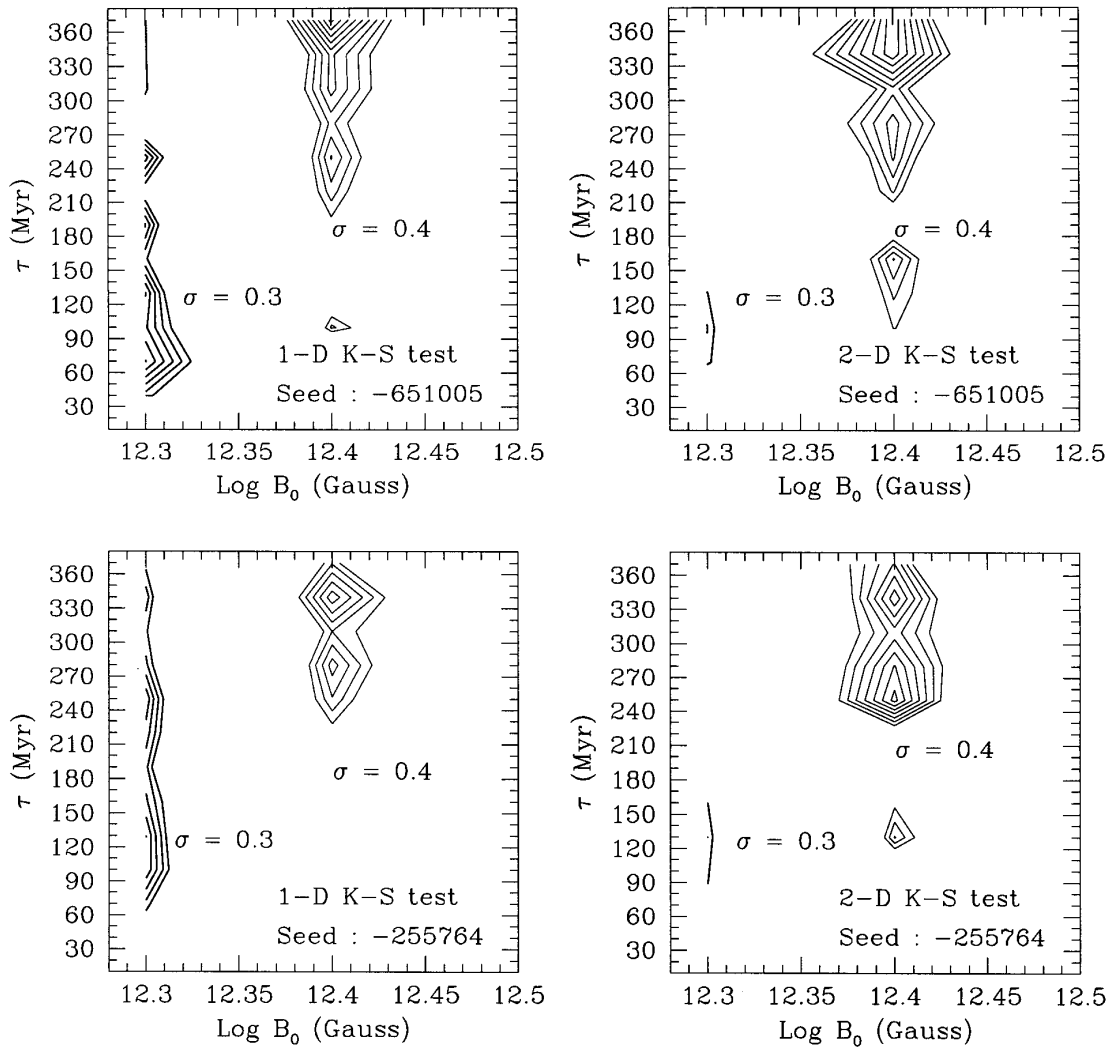

FIG. 2.—Equal probability contours in the log B_0-τ plane. Probability contours are shown for two values of $\sigma_{\log B_0}$ (0.3, 0.4), for two seed values, and for one- and two-dimensional K-S tests. Stollman's luminosity law and a velocity dispersion of 200 km s^{-1} were used.

from the tables that the $\tau \geq 200$ Myr is the most frequently reproduced value that gives the best-fit solution. It is clear from Figures 1 and 2 that properties such as the period, the period derivative, the magnetic field, and the luminosity are simultaneously well reproduced for the value of $\tau > 200$ Myr. However, *none* of the above mentioned properties could be matched with the observed sample for $\tau \sim 10$ Myr. It is difficult (and perhaps meaningless) to pinpoint an exact value of τ when the model is that of a truncated joint distribution having so many parameters. However, it is of considerable significance to note that in *all* the sets of simulations that we have carried out, we have obtained a *consistent lower bound* for τ. In a former study, Wakatsuki et al. (1992) proposed a constant field model as the better alternative to a decaying model (exponential or power law). However, exponential decay with timescale ≥ 160 Myr signifies practically no field decay at all during the active lifetime and hence cannot be distinguished from a truly constant magnetic field with the data presently available. We would, however, like to add that experimenting with the parameters (*a* and *b*) in the calculation of L_{400} will lead to a much wider range of acceptable values of τ (Hartman et al. 1997). We intend to include this effect in a subsequent study.

We have used the Taylor & Cordes (1993) distance model to calculate the dispersion measure. However, we find that the DM sin *b* factor is not well reproduced in any of the simulations. This is a bit surprising, since we have seen that this distance model takes into account all relevant factors of the structure of the Galaxy. In fact, the reason that Bhattacharya et al. (1992) obtained 130 pulsars in the selected observed sample (with 3 kpc cut off in the projected distance on the Galactic plane) while only 97 pulsars were included in the present study is that the distance estimates obtained from the old distance model (Lyne et al. 1985), as used by Bhattacharya and coworkers, were considerably lower than the most recent estimates given in the Taylor & Cordes (1993) model. This is also demonstrated in Figure 7, which shows that most of the pulsar distances were underestimated in the earlier model (Lyne et al. 1985).

As mentioned earlier, we are in the process of carrying out similar simulations that take into account the motion of pulsars in three dimensions. Preliminary studies with 200 and 500 simulated pulsars show the same trends as discussed in this paper.

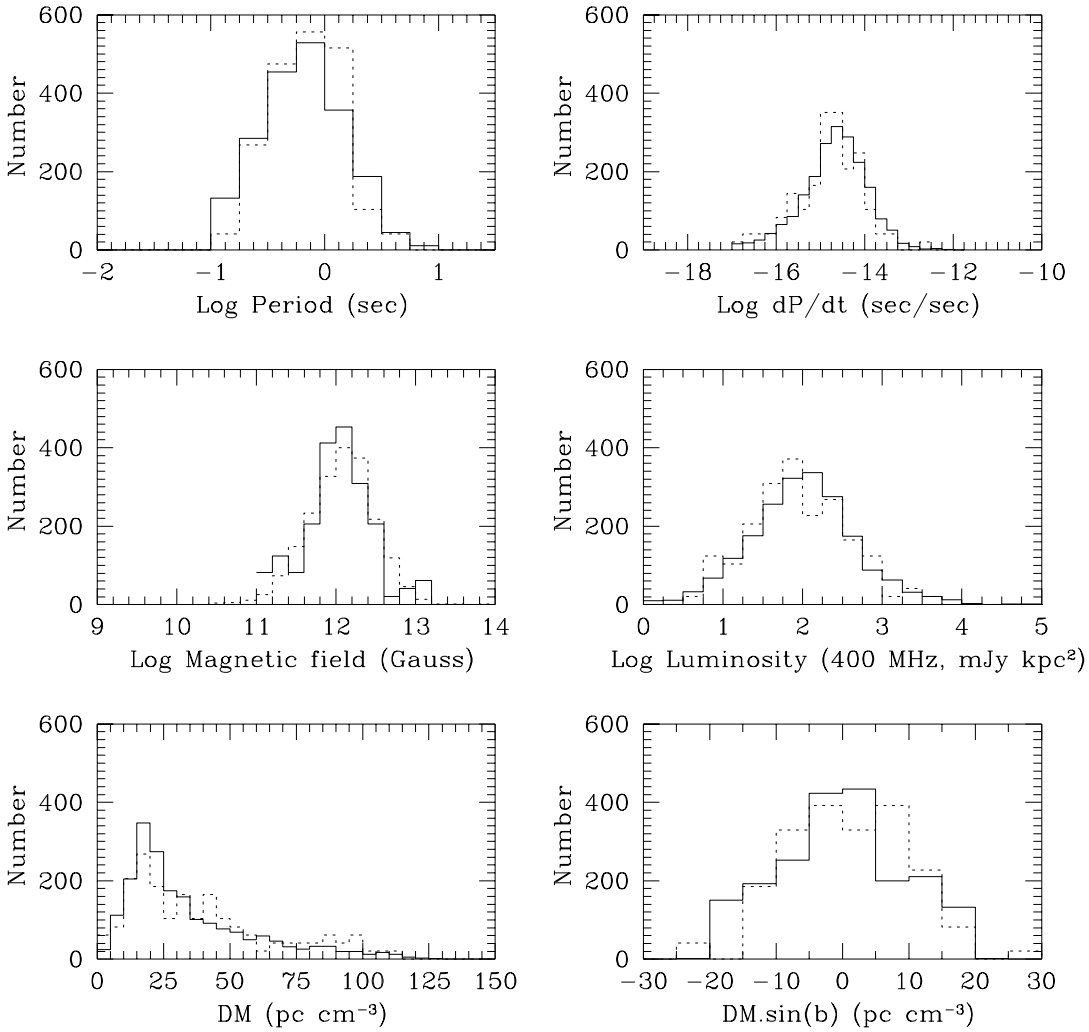

FIG. 3.—Distribution of the various properties of the simulated and observed pulsars after selection, for parameter values that give a good match. The solid lines show simulated and selected pulsars, while the dotted lines show observed and selected pulsars. Parameter values use in this simulation were log $B_0 = 12.4$, $\sigma_{\log B_0} = 0.4$, and $\tau = 280$ Myr. Stollman's luminosity law was used, and the number of simulated and selected pulsars was 2000.

The assumption regarding the uniform distribution of the age of the pulsars should be critically examined. This is because the existence of a correlation between the present pulsar distribution and the estimated locations of the spiral arms at earlier epochs (Ramachandran & Deshpande 1994) might be a crucial factor in influencing birthrates. This has not been modeled in the present simulation but would be important in any future study.

Last, we would like to include a detailed discussion regarding the justification of the choice of step size in the variation of log B_0 and σ in the simulation. The choice of the step size of the variables has an important effect on the inference that we draw on the field decay constant, τ, and thus a thorough discussion on the various aspects of it is relevant. As is explained in § 4.3, we started by varying log B_0 and σ over a very fine grid of parameter space, as in Bhattacharya et al. (1992) and Hartman et al. (1997). However, we found that the best-fit values obtained were strongly correlated for such fine variation of the parameters. The fit was indeed equally good everywhere. We described this as "insensitive to small step variations" and decided to use larger steps ($=0.1$) that led to stable peak probability values and also reduced the computation load to a large extent. We shall show in a subsequent paper (which is about to be communicated) that if we retain parameter variation over such fine grid, a much wider range of acceptable value of τ can be obtained. However, we feel that caution must be taken in the interpretation of this result, since what might appear to give more acceptable values of τ might actually be caused by statistical noise fluctuations. As we can see, the whole model is a complex one with the inclusion of many parameters and variables. The quantity τ is not a monotonic function of these variables, nor is the dependence of τ on these parameters a predictable one. This aspect tends to add to the statistical noise associated with complex numerical simulations, such as those undertaken in the present study. However, it is also important to note that noise is present in any real data set, and one should allow enough degrees of freedom so as not to suppress it as far as possible. In Figure 2, we have plotted the probability contours as

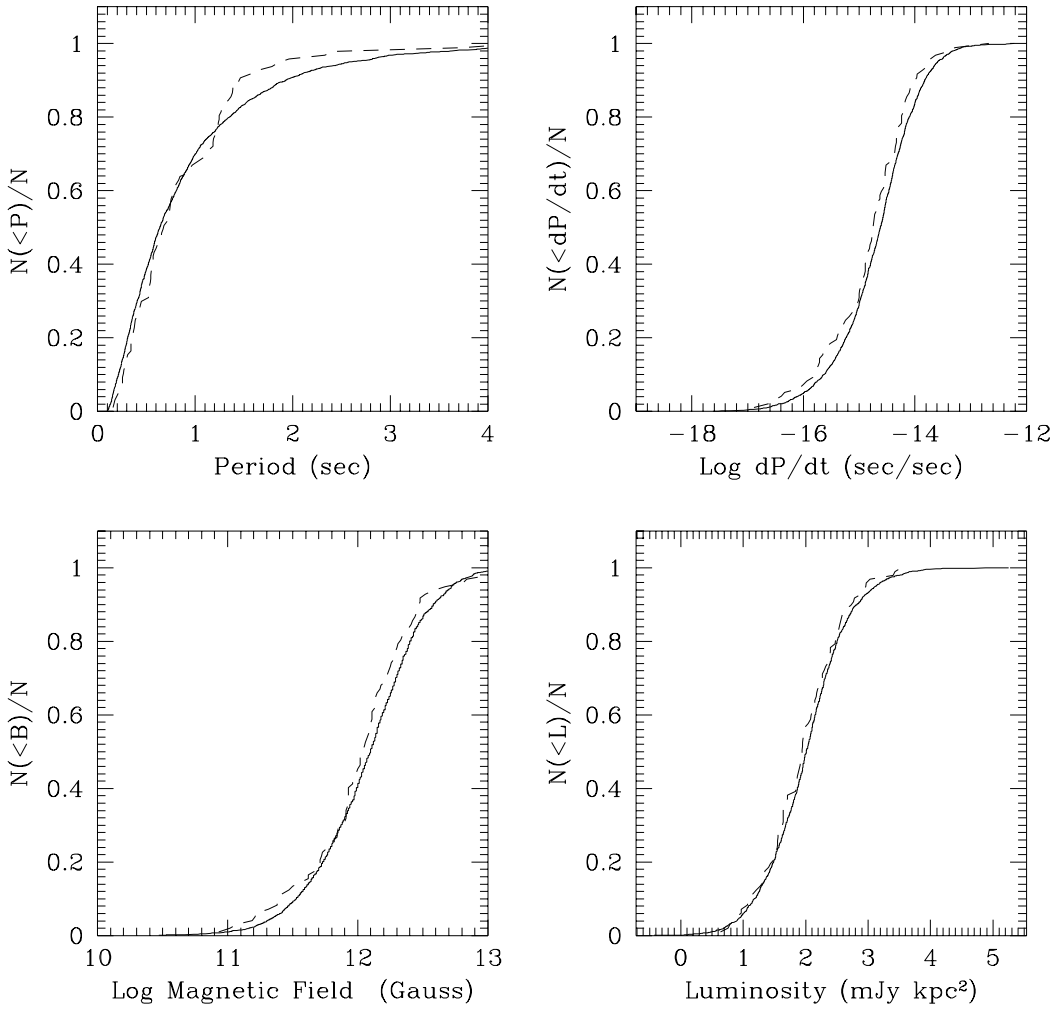

FIG. 4.—Cumulative distribution of various properties of simulated and observed pulsars after selection. Details are as in Fig. 3.

obtained from the results of our repeated simulations using different seed values using the above criterion of the choice of grids. In the earlier study by Bhattacharya et al. (1992), a contour level of $1/e^2$ below the maximum on the grid was used, and the authors found that its location was fairly stable to the variations of the seed. This is a clear alternative way of defining the area of best fit.

To conclude, we stress that inclusion of the most recent distance and velocity estimates make our simulations more realistic than the previous studies. We also avoid selecting the x- and y-position coordinates from a uniform distribution around the Sun (which was a doubtful assumption as pointed out in B92), generate the coordinates from appropriate distributions as explained in § 2, and evolve them under the Galactic potential. We have used a more detailed form of this potential (Lorimer 1995) than used in any of the previous simulations of a similar nature. We have also taken into account Galactic rotation in solving the equations of motion in order to model the pulsar position with as much accuracy as possible. The use of a two-dimensional Kolmogorov-Smirnov test to examine the distributions of the pulsars in the B-P and P–DM sin b planes provides a more sensitive indicator for the comparision of distributions than the one-dimensional tests used so far. The present study confirms the result of Bhattacharya et al. (1992) that there is no significant field decay in single radio pulsars during their active lifetime.

The authors thank E. P. J. van den Heuvel, Frank Verbunt, Yashwant Gupta, M. Vivekanand, and, particularly, Dipankar Bhattacharya for many helpful discussions and Ralph Wijers for valuable comments. The authors acknowledge Anup Dewanji and Probal Chaudhuri for useful comments and suggestions and for constructive criticism regarding the statistical analysis. The authors acknowledge Professors Anil Gore and S. Kunte for helpful discussions regarding statistics. S. M. would like to express thanks to Partha Pramanik of Computer and Statistical Service Centre, Indian Statistical Institute, Calcutta for the cooperation extended during the initial stages of computation and to the Inter-University Centre for Astronomy and Astrophysics for funding several visits during which this paper was completed.

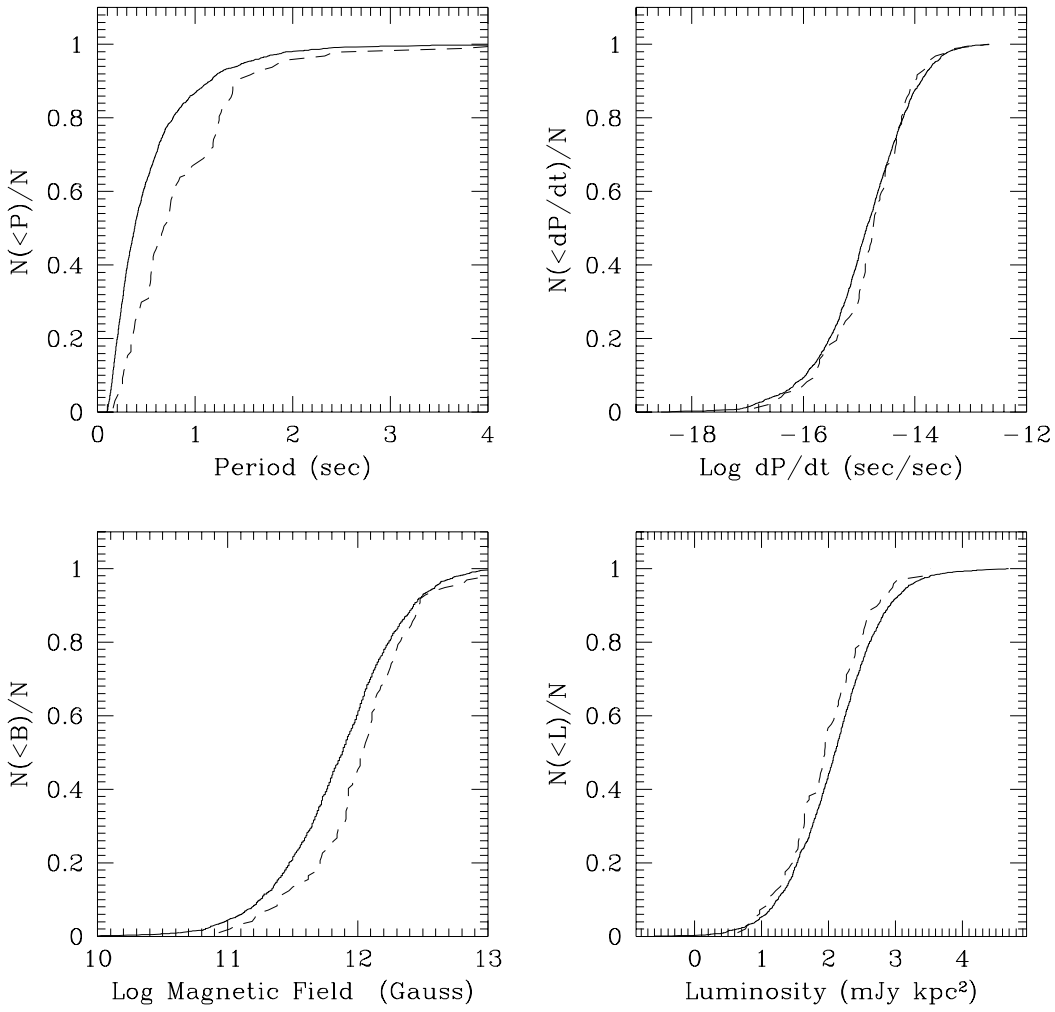

FIG. 5.—The cumulative distribution of various properties as in Fig. 4 but for $\tau = 10$ Myr. The mismatch between observation and simulation for this low value of the magnetic field decay timescale is clearly seen.

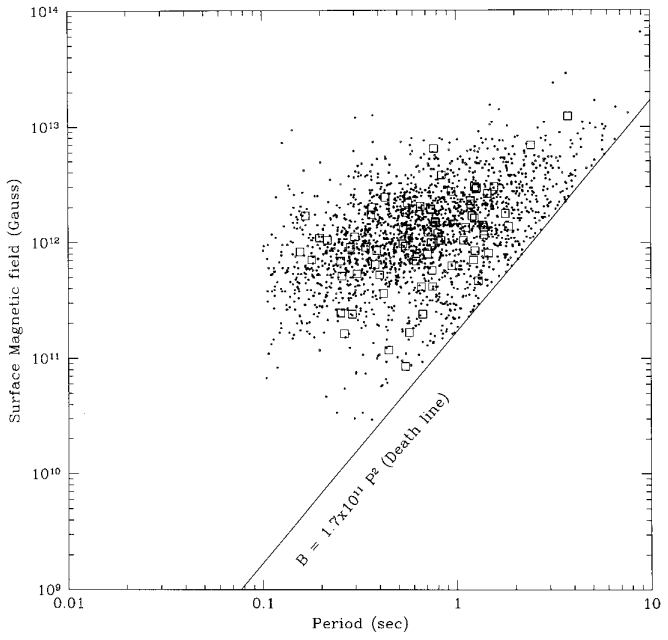

FIG. 6.—Distribution of pulsars on the *B-P* plane. The dots represent the simulated and selected pulsars, while the squares represent observed and selected pulsars.

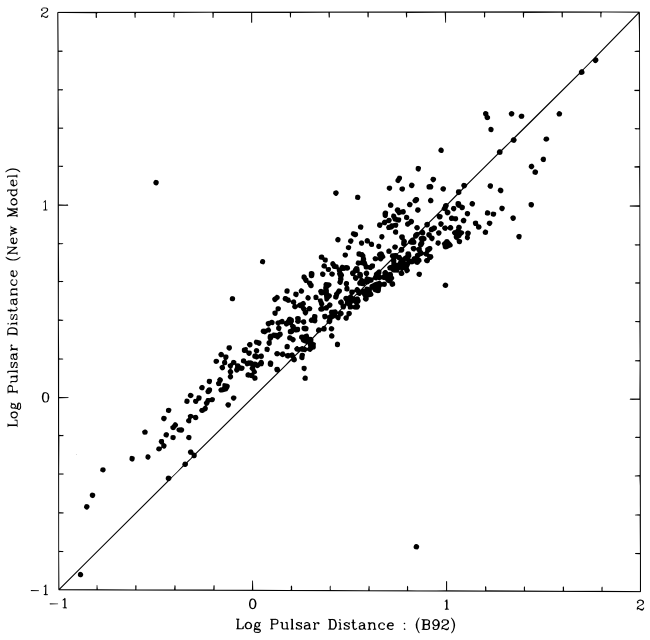

FIG. 7.—Comparision of pulsar distances obtained using the new distance model and as in Bhattacharya et al. (1992). The distances are in kiloparsecs.

REFERENCES

Bailes, M. 1989, ApJ, 342, 917
Bhattacharya, D., & Srinivasan, G. 1991, in Neutron Stars: Theory and Observations, ed. J. Ventura & D. Pines (Dordrecht: Kluwer), 219
Bhattacharya, D., & van den Heuvel, E. P. J. 1991, Phys. Rep., 203, 1
Bhattacharya, D., Wijers, R. A. M. J., Hartman, J. W., & Verbunt, F. 1992, A&A, 254,198
Carlberg, R. G., & Innanen, K. A. 1987, AJ, 94, 666
Damashek, M., Taylor, J. H., & Hulse, R. A. 1978, ApJ, 225, L31
Davies, J. G., Lyne, A. G., & Seiradakis, J. H. 1972, Nature, 240, 229
Dewey, R. J., Stokes, G. H., Segelstein, D. J., Taylor, J. H., & Weisberg, J. M. 1984, Millisecond Pulsars, ed. S. P. Reynolds & D. R. Stinebring (Greenbank: NRAO), 234
Fasano, G., & Franceschini, A. 1987, MNRAS, 225, 155
Fomalont, E. B., Goss, W. M., Lyne, A. G., Manchester, R. N., & Justtanont, K. 1992, MNRAS, 258, 497
Gunn, J. E., & Ostriker, J. P. 1970, ApJ, 160, 979
Harrison, P. A., Lyne, A. G., & Anderson, B. 1993, MNRAS, 261, 113
Hartman, J. W., Bhattacharya, D., Wijers, R. & Verbunt, F. 1997, A&A, in press
Haslam, C. G. T., Salter, C. J., Stoffel, H., & Wilson, W. E. 1982, A&AS, 47, 1
Helfand, D., & Tademaru, E. 1977, ApJ, 216, 842
Hulse, R. A., & Taylor, J. H. 1974, ApJ, 191, L59
Lorimer, D. 1995, Ph.D. thesis, Univ. of Manchester
Lyne, A. G., Anderson, B., & Salter, M. J. 1982, MNRAS, 201, 503
Lyne, A. G., & Lorimer, D. 1994, Nature, 369, 127
———. 1995, J. Astrophys. Astron., 16, 97
Lyne, A. G., & Manchester, R. N. 1988, MNRAS, 234, 477
Lyne, A. G., Manchester, R. N., & Taylor, J. H. 1985, MNRAS, 213, 613
Manchester, R. N., Lyne, A. G., Taylor, J. H., Durdin, J. M., Large, M. I., & Little, A. G. 1978, MNRAS, 185, 409
Mihalas, D., & Binney, J. 1981, Galactic Astronomy (San Francisco: Freeman)
Narayan, R. 1987, ApJ, 319, 162
Narayan, R., & Ostriker, J. P. 1990, ApJ, 352, 222
Narayan, R., & Vivekanand, M. 1983, A&A, 122, 45
Ostriker, J. P., & Gunn, J. E. 1969, ApJ, 157, 1395
Peacock, J. A. 1983, MNRAS, 202, 615
Press, X., et al. 1992, Numerical Recipes (2d ed; Cambridge: Cambridge Univ. Press)
Proszynski, M., & Przybycien, D. 1984, Millisecond Pulsars, ed. S. P. Reynolds & D. R. Stinebring (Greenbank: NRAO), 234
Ramachandran, R., & Deshpande, A. A. 1994, J. Astro. Astron., 15, 69
Rankin, J. M. 1990, ApJ, 352, 247
Rawley, L. A., Taylor, J. H., & Davis, M. M. 1986, Nature, 319, 383
Romani, R. W. 1990, Nature, 347, 741
Ruderman, M. A., & Sutherland, P. G. 1975, ApJ, 196, 51
Sang, Y., & Chanmugam, G. 1987, ApJ, 323, L61
———. 1990, ApJ, 363, 597
Stollman, G. M. 1986, A&A, 171, 152
Taylor, J. H., & Cordes, J. M. 1993, ApJ, 411, 674
Taylor, J. H., Manchester, R. N., Lyne, A. G., & Camilo, F. 1995, Catalog of 706 Pulsars (Princeton: Princeton Univ. Press)
Taylor, J. H., & Stinebring, D. R. 1986, ARA&A, 24, 285
Wakatsuki, S., Hikita, A., Sato, N., & Itoh, N. 1992, ApJ, 392,628